

Deliverable 3.2: Development of surface passivation

In this workpackage we investigate the surface passivation of Hex-Ge and Hex-SiGe nanowire shells in order to reduce the expected non-radiative losses due to dangling bonds at the surface.

The emission properties of cubic germanium are known to be highly sensitive to pre-treatment of the surface. Since the surface chemistry of cubic Ge and Hex-Ge will probably be comparable, we expect to be able to push the room temperature emission intensity of our Hex-Ge nanowires by several orders of magnitude.

We investigate two approaches to passivate the surface of Hex-Ge. Firstly we try to passivate the Hex-Ge directly by pre-treating the surface and depositing a large bandgap oxide to passivate and protect the surface. The second approach is to grow a very thin epitaxial layer of Si around the Hex-Ge shell. If needed this Si-shell can subsequently be passivated again using well known atomic layer deposition (ALD) techniques. In addition to the direct passivation of pure Ge we will also separately optimize the passivation of SiGe alloys. The surface of this material can be both Si-like and Ge-like and might therefore need a customized approach which passivates both.

Direct passivation of Ge and SiGe nanowires

It is very well known that a thermally grown oxide on Si provides an excellent passivation layer for Si. Unfortunately the natural oxide of Ge is soluble in water [1], [2] and has a limited thermal stability [1], [3]–[5], therefore it is considered unsuitable in an ambient environment. However when covered by a protective layer, GeO_x still holds great promise for passivating the surface of Ge and Ge-rich alloys[6], [7].

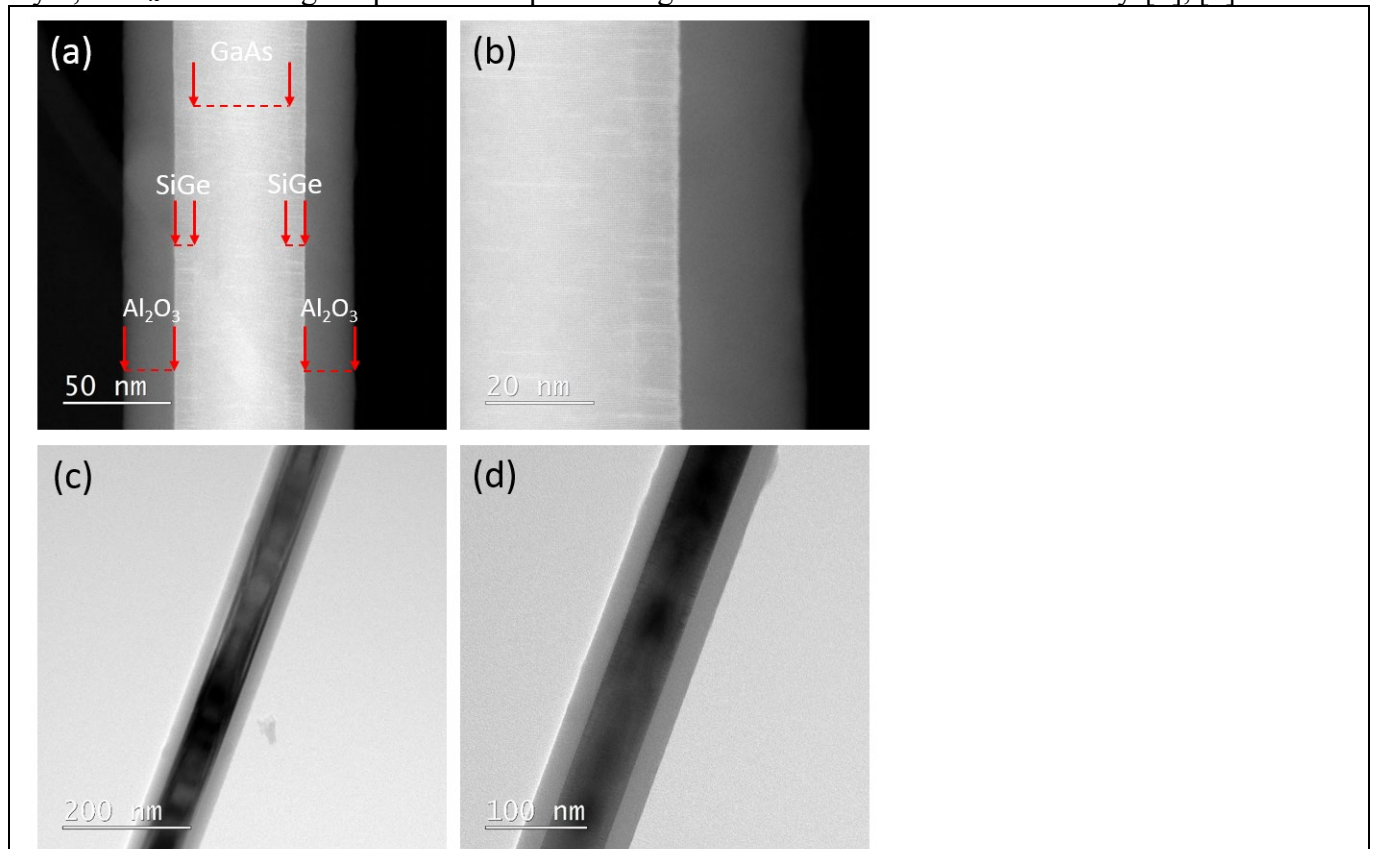


Figure 3.2.1 (a) and (b) show HAADF TEM images of a GaAs/SiGe/ AlO_x core/shell/shell structure. The ALD grown AlO_x formed a very homogeneous layer over the wire. (c) and (d) show bright field TEM images under the $\langle 0110 \rangle$ and $\langle 2110 \rangle$ zone axis respectively, indicating no preferential growth of AlO_x on different facets.

Concerning the pre-ALD passivation treatment optimization, we will explore several methods of oxidizing the surface of Ge and SiGe including native oxide, plasma-assisted oxidation and ozone assisted oxidation. After which the oxide will be capped with an amorphous layer of AlO_x which has proven to give excellent passivation for crystalline Si. Also we will probe the effects of directly passivating the Ge and SiGe surface with AlO_x by first stripping the native oxides from the SiGe alloys using an appropriate etchant such as Hydrofluoric acid (HF) or Hydrochloric acid (HCl) after which AlO_x will be deposited using ALD.

A first important step was taken in succeeding to deposit a homogeneous amorphous layer of AlO_x on GaAs/SiGe core/shell nanowires. Using a low temperature ALD technique with TMA and O_2 as precursors a layer of 20 nm was successfully deposited. To verify the successful growth, transmission electron microscopy (TEM) was used to characterise some of the passivated wires. In Fig. 3.2.1 (a) and (b) HAADF images are shown in which in (a) the different layers are indicated with arrows. Due to the similar atomic masses of Ga, As and Ge only a very small contrast can be deduced between the core and the SiGe shell. The preserved crystallinity of the GaAs-core and the SiGe-shell is imaged in Fig. 3.2.1 (b) where the diffuse contrast of the AlO_x indicates that the ALD-deposited layer is indeed amorphous.

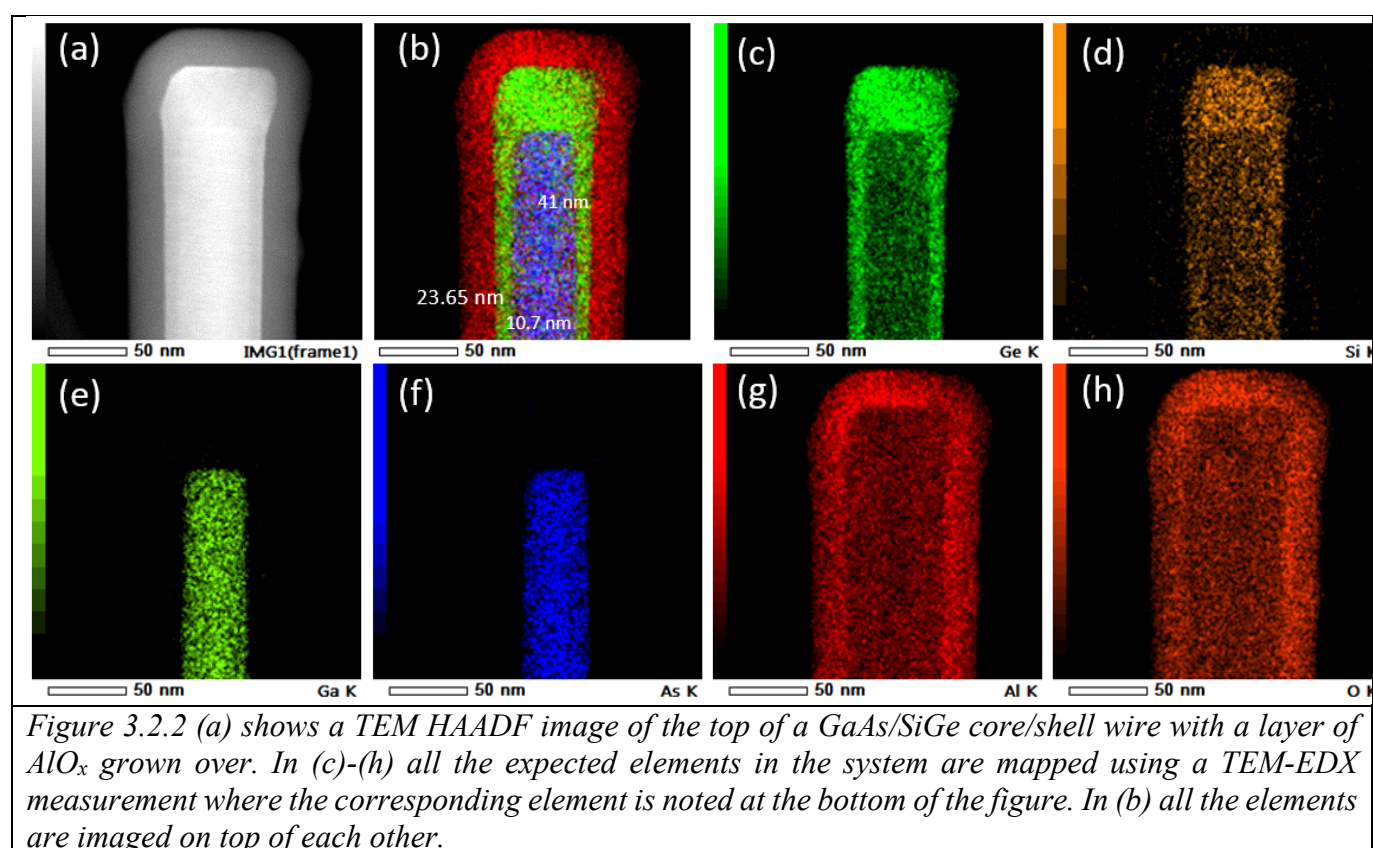


Fig. 3.2.1 (c) and (d) are TEM bright field images measured under different zone-axis of the wire. From these we can deduce that the AlO_x layer has no preference for facets on the SiGe shell but grows with an equal speed in all directions. During the AlO_x deposition a Ge wafer was also placed in the reactor from which the layer thickness could be measured *in situ*. This showed us that there is no significant nucleation time and that the thickness on cubic Ge increased linearly with longer deposition.

An advantage of the low temperature deposition method of ALD is that diffusion is strongly suppressed, to verify Energy-dispersive X-ray spectroscopy (XPS) measurements were performed as shown in Fig. 3.2.2. Here all the elements in the structure are individually mapped, showing a clear contrast between the GaAs core and the SiGe shell. It is also clear that there is a homogeneous distribution of aluminium and oxide in the amorphous capping layer and that there are no enrichments of either.

For initial passivation experiments an extensive set of samples has been grown. One set of identical GaAs/Ge nanowire samples has been grown in a single MOVPE reactor run to avoid any discrepancy

between them. Also a batch of GaAs/SiGe nanowire samples has been grown in a similar fashion. After the growth of the hexagonal group-IV shells the samples were taken out of the MOVPE reactor and undergone a treatment of either; no treatment, a diluted 1% HF dip or a UV ozone treatment. Following this pre-treatment the samples were loaded as quickly as possible into the ALD reactor and a 20 nm shell of amorphous AlO_x was grown to protect the Hex-SiGe shells.

From the literature of Si passivation with AlO_x it is well known [8], [9] that a post-deposition annealing step is crucial for the activation of the passivation. The role of this annealing step is understood as a thermally activated breaking of O-H bonds which are present in the AlO_x layer. The annealing step subsequently allows the atomic hydrogen to diffuse to the interface and bind to dangling bonds of the silicon crystal. This process is well documented for cubic Si and an optimal annealing temperature of 425°C is established. However, since both the diffusion as well as the binding of the atomic hydrogen is a temperature controlled process, an optimal annealing temperature might be different for germanium rich alloys or pure germanium. To re-optimize this temperature for our system a series of AlO_x passivated samples was prepared and annealed at different temperatures both for Hex-SiGe shells as well as for Hex-Ge shells.

Optical characterization of direct passivation

To test and compare the quality of our passivation schemes, Fast Fourier Transform InfraRed (FTIR) photoluminescence (PL) spectroscopy is a straightforward choice. From the large batch of samples available, we have chosen to start with the optimization of the annealing temperature. This provides the opportunity to later anneal differently pre-treated samples at the ideal conditions, and such, make the best comparison between them. Initial characterizations have been carried out on the GaAs/ $\text{Si}_{0.23}\text{Ge}_{0.77}$ core-shell nanowires which emit at a more favourable wavelength for quick feedback than pure germanium structures. The samples have been mounted in a helium-flow cryostat and were cooled down to 4 K for initial characterisation. A 976 nm CW laser was used as excitation source, which was modulated at 100 kHz to partially avoid heating. The PL signal was coupled into an FTIR using all mirror optics and measured using an extended InGaAs detector.

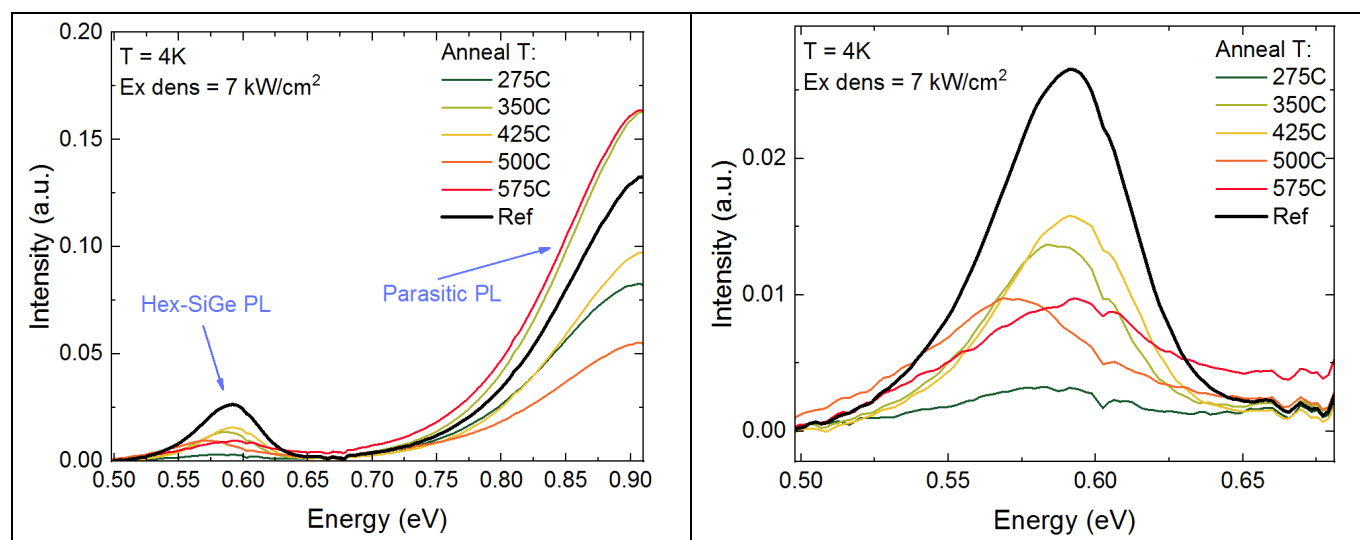
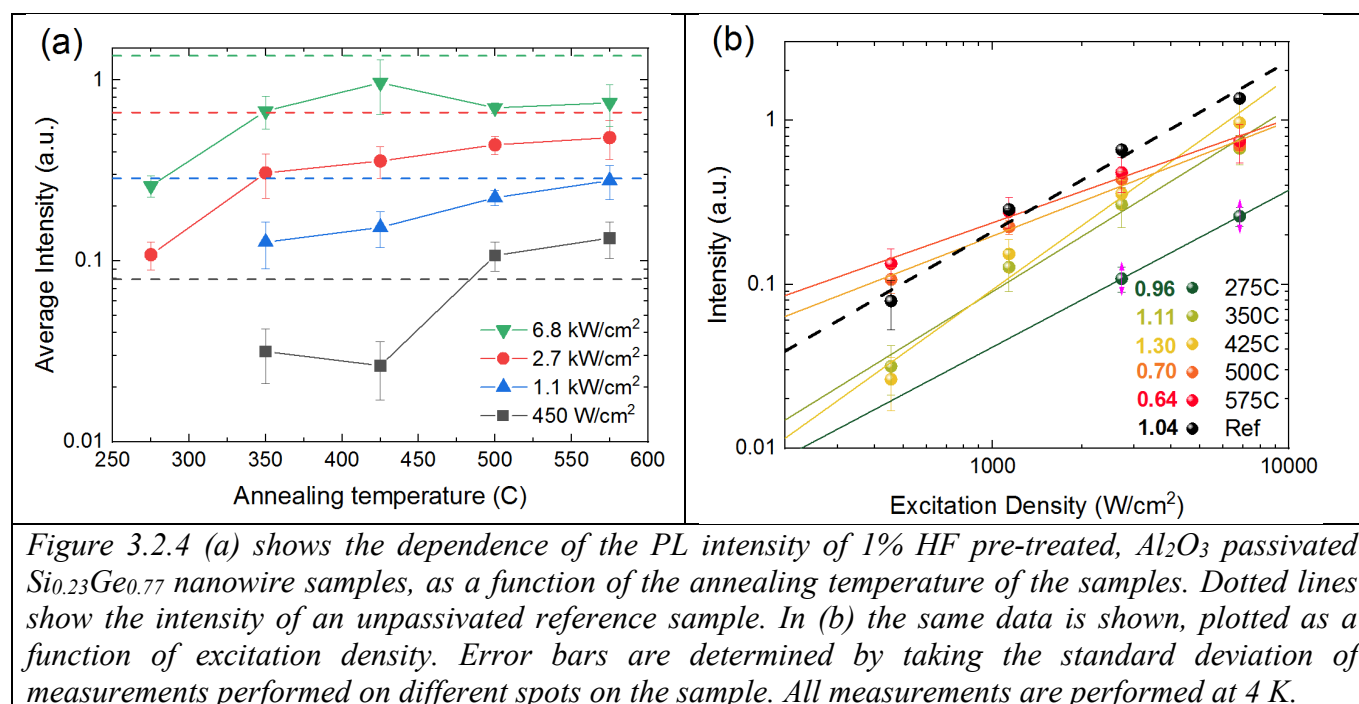


Figure 3.2.3 (a) shows the PL spectra of 1% HF pre-treated, Al_2O_3 passivated $\text{Si}_{0.23}\text{Ge}_{0.77}$ nanowires, annealed at different temperatures at high excitation density. (b) shows a zoom-in of (a) where the PL originating from the hex- $\text{Si}_{0.23}\text{Ge}_{0.77}$ part can be compared.

Measured PL spectra of Hex- $\text{Si}_{0.23}\text{Ge}_{0.77}$ samples are shown in Fig. 3.2.3 (a) and (b). The spectrum consists out of a small PL peak around 0.59 eV, which can be unambiguously attributed to the SiGe shell because of the observed gradual shift of the emission energy when increasing the silicon content as described in **deliverable 2.1**. The small energy differences between the spectra as seen in Fig. 3.2.3 (b) can be explained by small local differences in alloying. Additionally, the spectrum shows a parasitic peak around 0.9 eV which is most probably related to the unintentional growth of cubic SiGe on the planar GaAs substrate.



Although a proper passivation is expected to have a much larger effect at higher temperatures due to the thermal activation of traps, a first characterisation is carried out at liquid helium temperatures to identify the surface effects in a low-loss regime. In Fig. 3.2.4 (a) the dependence of the PL intensity of the passivated Si_{0.23}Ge_{0.77} nanowire shells on the annealing temperature is plotted for different excitation densities. The PL intensity is clearly influenced by the annealing temperature of the samples which verifies the relevance of surface passivation for this material system.

For all excitation densities a continuous increase of the PL intensity is measured for increasing annealing temperature, with the surprising exception of the highest excitation density. For this excitation of 6.8 kW/cm² an optimal annealing temperature of 425° C is found, which exactly matches the literature value for cubic Si. In Fig. 3.2.4 (b) the excitation density dependence for each sample is plotted showing a steepest increase for the sample annealed at 425°C which surprisingly performs almost worst at the lowest excitation density.

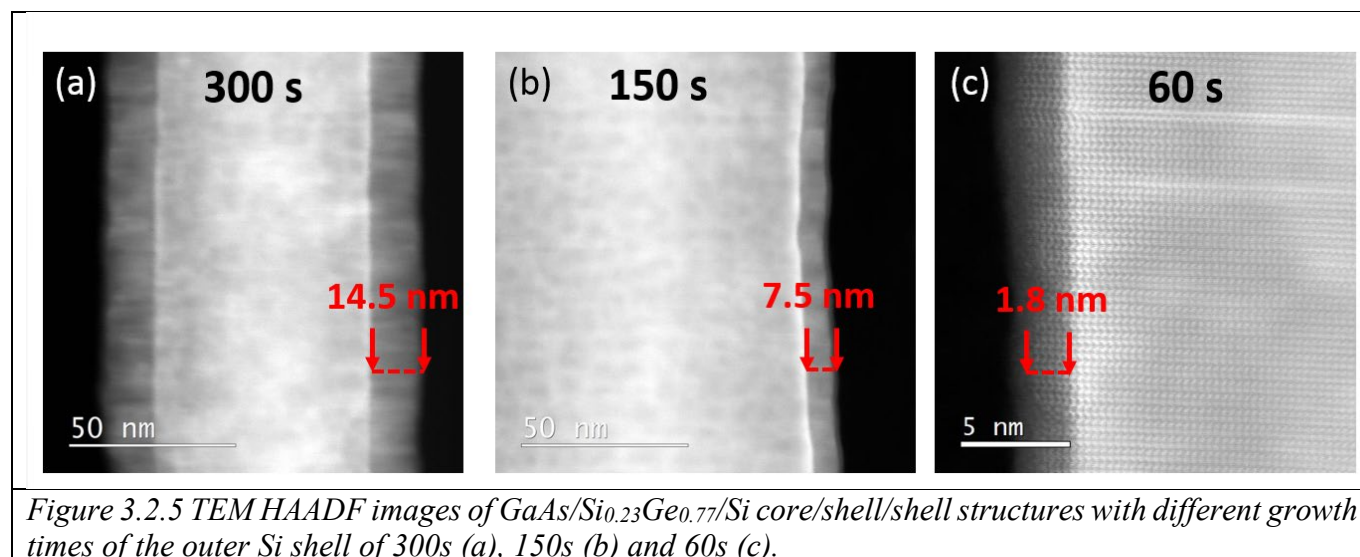
This performance discrepancy at different excitation densities can only be understood when more than a single competing surface loss-mechanism is taken into account. In the alloy we try to passivate, both unbound Si as well as Ge dangling bonds which can act as recombination centres with different activation energies. Since it is already known from literature that a Ge-H bond is much less stable than a Si-H bond it is expected that different treatments provide a different balance between these two loss mechanisms. In addition, surface-charge effects should also be taken into account, which are known to play a large role in the passivation of silicon [9].

To decouple different loss contributions, temperature dependent PL measurements will be carried out, which will not only amplify the passivation effect compared to an as-grown sample but also allow to derive the activation energies of the different loss canals. Additionally a similar measurement scheme will be used to characterize the properties of passivated Hex-Ge nanowires which will allow us to discriminate between Ge-like and Si-like loss-contributions.

Passivation using a thin epitaxial Silicon layer

A proven method of passivating germanium is by growing an epitaxial shell of Hex-Si to protect the surface and confine charge carriers into the germanium [10]–[12]. This method however relies on quantum confinement effects in the thin Si layer to overcome the problem of the type-II band-offset between Si and Ge. This makes its effectiveness highly dependent on the thickness of the silicon layer which should be controlled down to only a few a nanometres.

To pursue this approach, first experiments have been carried out to determine the growth rate and homogeneity of a Si-shell on Hex-Ge. For this purpose, a time series of three different times for the growth of Hex-Si around the Hex-Ge has been performed. As a first step, a Hex-Ge shell with the exact same thickness and growth conditions have been grown using Germane (GeH_4) as a Ge precursor. Subsequently, the GeH_4 was switched off and immediately the Si precursor, tetrasilane (Si_4H_{10}) was introduced for three different times 60, 150 and 300 seconds to investigate the growth of the Si layer. The thickness of the Si shells for samples with three different growth-times have been determined using TEM as depicted in Fig. 3.2.5. From this study, the nucleation time and growth-rate have been determined which will enable us to fine-tune the silicon thickness in future work.



References:

- [1] Q. Xie, S. Deng, M. Schaeckers, D. Lin, M. Caymax, A. Delabie, X. P. Qu, Y. L. Jiang, D. Deduytsche, and C. Detavernier, "Germanium surface passivation and atomic layer deposition of high-k dielectrics - A tutorial review on Ge-based MOS capacitors," *Semicond. Sci. Technol.*, vol. 27, no. 7, 2012.
- [2] T. Hanrath and B. A. Korgel, "Chemical surface passivation of Ge nanowires," *J. Am. Chem. Soc.*, vol. 126, no. 47, pp. 15466–15472, 2004.
- [3] K. Ikejiri, Y. Kitauchi, K. Tomioka, J. Motohisa, and T. Fukui, "Zinc blende and wurtzite crystal phase mixing and transition in indium phosphide nanowires," *Nano Lett.*, vol. 11, no. 10, pp. 4314–4318, 2011.
- [4] K. Kita, S. Suzuki, H. Nomura, T. Takahashi, T. Nishimura, and A. Toriumi, "Direct evidence of GeO volatilization from GeO₂/Ge and impact of its suppression on GeO₂/Ge metal-insulator-semiconductor characteristics," *Jpn. J. Appl. Phys.*, vol. 47, no. 4 PART 2, pp. 2349–2353, 2008.
- [5] K. Prabhakaran, F. Maeda, Y. Watanabe, and T. Ogino, "Distinctly different thermal decomposition pathways of ultrathin oxide layer on Ge and Si surfaces," *Appl. Phys. Lett.*, vol. 76, no. 16, pp. 2244–2246, 2000.
- [6] Y. Fukuda, T. Ueno, S. Hirono, and S. Hashimoto, "Electrical characterization of germanium oxide/germanium interface prepared by electron-cyclotron-resonance plasma irradiation," *Japanese J. Appl. Physics, Part 1 Regul. Pap. Short Notes Rev. Pap.*, vol. 44, no. 9 B, pp. 6981–6984, 2005.
- [7] H. Matsubara, T. Sasada, M. Takenaka, and S. Takagi, "Evidence of low interface trap density in Ge O₂ Ge metal-oxide-semiconductor structures fabricated by thermal oxidation," *Appl. Phys. Lett.*, vol. 93, no. 3, pp. 91–94, 2008.
- [8] B. Hoex, J. Schmidt, P. Pohl, M. C. M. Van De Sanden, and W. M. M. Kessels, "Silicon surface passivation by atomic layer deposited Al₂O₃," *J. Appl. Phys.*, vol. 104, no. 4, 2008.
- [9] G. Dingemans, R. Seguin, P. Engelhart, M. C. M. van de Sanden, and W. M. M. Kessels, "Silicon surface passivation by ultrathin Al₂O₃ films synthesized by thermal and plasma atomic layer deposition," *Phys. Status Solidi - Rapid Res. Lett.*, vol. 4, no. 1–2, pp. 10–12, 2010.
- [10] R. Pillarisetty, B. Chu-Kung, S. Corcoran, G. Dewey, J. Kavalieros, H. Kennel, R. Kotlyar, V. Le, D. Lionberger, M. Metz, N. Mukherjee, J. Nah, W. Rachmady, M. Radosavljevic, U. Shah, S. Taft, H. Then, N. Zelick, and R. Chau, "High mobility strained germanium quantum well field effect transistor as the P-channel device option for low power (V_{cc} = 0.5 V) III-V CMOS architecture," *Tech. Dig. - Int. Electron Devices Meet. IEDM*, pp. 150–153, 2010.
- [11] D. P. Brunco, B. De Jaeger, G. Eneman, J. Mitard, G. Hellings, A. Satta, V. Terzieva, L. Souriau, F. E. Leys, G. Pourtois, M. Houssa, G. Winderickx, E. Vrancken, S. Sioncke, K. Opsomer, G. Nicholas, M. Caymax, A. Stesmans, J. Van Steenberghe, P. W. Mertens, M. Meuris, and M. M. Heyns, "Germanium MOSFET Devices: Advances in Materials Understanding, Process Development, and Electrical Performance," *J. Electrochem. Soc.*, vol. 155, no. 7, p. H552, 2008.
- [12] M. Caymax, F. Leys, J. Mitard, K. Martens, L. Yang, G. Pourtois, W. Vandervorst, M. Meuris, and R. Loo, "The Influence of the Epitaxial Growth Process Parameters on Layer Characteristics and Device Performance in Si-Passivated Ge pMOSFETs," *J. Electrochem. Soc.*, vol. 156, no. 12, p. H979, 2009.